

# Geochemistry, Geophysics, Geosystems®

## RESEARCH ARTICLE

10.1029/2024GC011583

Cindy De Jonge and Francien Peterse contributed equally to this work.

### Key Points:

- 39 laboratories participated in a round robin to determine the reproducibility of glycerol dialkyl glycerol tetraethers (GDGT) proxy values and quantities
- Peak selection impacts the ratio values and there is no apparent systematic impact of the extraction method and sample preparation steps
- Quantification of GDGTs remains a problem, and comparison of GDGT concentrations between laboratories requires further method development

### Supporting Information:

Supporting Information may be found in the online version of this article.

### Correspondence to:

C. De Jonge,  
cindy.dejonge@erdw.ethz.ch

### Citation:

De Jonge, C., Peterse, F., Nierop, K. G. J., Blattmann, T. M., Alexandre, M., Ansanay-Alex, S., et al. (2024). Interlaboratory comparison of branched GDGT temperature and pH proxies using soils and lipid extracts. *Geochemistry, Geophysics, Geosystems*, 25, e2024GC011583. <https://doi.org/10.1029/2024GC011583>

Received 26 MAR 2024

Accepted 26 JUN 2024

© 2024 The Author(s). *Geochemistry, Geophysics, Geosystems* published by Wiley Periodicals LLC on behalf of American Geophysical Union.

This is an open access article under the terms of the [Creative Commons Attribution License](#), which permits use, distribution and reproduction in any medium, provided the original work is properly cited.

## Interlaboratory Comparison of Branched GDGT Temperature and pH Proxies Using Soils and Lipid Extracts

Cindy De Jonge<sup>1</sup> , Francien Peterse<sup>2</sup> , Klaas G. J. Nierop<sup>2</sup>, Thomas M. Blattmann<sup>1</sup> , Marcelo Alexandre<sup>3</sup>, Salome Ansanay-Alex<sup>4</sup>, Thomas Austin<sup>5</sup> , Mathieu Babin<sup>6</sup>, Edouard Bard<sup>7</sup> , Thorsten Bauersachs<sup>8,9</sup> , Jerome Blewett<sup>10</sup>, Brenna Boehman<sup>11</sup> , Isla S. Castañeda<sup>12</sup>, Junhui Chen<sup>13</sup>, Martina L. G. Conti<sup>14</sup> , Sergio Contreras<sup>15</sup> , Julia Cordes<sup>16</sup>, Nina Davtian<sup>17</sup> , Bart van Dongen<sup>18</sup> , Bella Duncan<sup>19</sup>, Felix J. Elling<sup>20</sup> , Valier Galy<sup>11</sup> , Shaopeng Gao<sup>21</sup> , Jens Hefter<sup>22</sup> , Kai-Uwe Hinrichs<sup>16</sup> , Mitchell R. Helling<sup>23</sup> , Mariska Hoorweg<sup>2</sup>, Ellen Hopmans<sup>24</sup> , Juzhi Hou<sup>21</sup> , Yongsong Huang<sup>3</sup> , Arnaud Huguet<sup>25</sup> , Guodong Jia<sup>26</sup>, Cornelia Karger<sup>27</sup>, Brendan J. Keely<sup>14</sup>, Stephanie Kusch<sup>6</sup> , Hui Li<sup>26</sup>, Jie Liang<sup>21</sup> , Julius S. Lipp<sup>16</sup>, Weiguo Liu<sup>28</sup> , Hongxuan Lu<sup>28</sup> , Kai Mangelsdorf<sup>27</sup> , Hayley Manners<sup>29</sup> , Alfredo Martinez Garcia<sup>30</sup> , Guillemette Menot<sup>4</sup> , Gesine Mollenhauer<sup>22</sup> , B. David A. Naafs<sup>31</sup> , Sebastian Naehler<sup>5</sup> , Lauren K. O'Connor<sup>18,32</sup> , Ethan M. Pearce<sup>14</sup> , Ann Pearson<sup>10</sup> , Zhiguo Rao<sup>33</sup> , Marta Rodrigo-Gámiz<sup>34</sup> , Chris Rosendahl<sup>20</sup>, Frauke Rostek<sup>7</sup>, Rui Bao<sup>35</sup> , Prasanta Sanyal<sup>36</sup> , Florence Schubotz<sup>16</sup> , Wesley Scott<sup>37</sup>, Rahul Sen<sup>36</sup>, Appy Sluijs<sup>2</sup> , Rienk Smittenberg<sup>38,39</sup> , Ioana Stefanescu<sup>40</sup> , Jia Sun<sup>31</sup>, Paul Sutton<sup>29</sup> , Jess Tierney<sup>41</sup> , Eduardo Tejos<sup>15</sup> , Joan Villanueva<sup>17</sup> , Huanye Wang<sup>28</sup> , Josef Werne<sup>38</sup> , Masanobu Yamamoto<sup>42</sup> , Huan Yang<sup>43</sup> , and Aifeng Zhou<sup>44</sup> 

<sup>1</sup>Geological Institute, ETH Zürich, Zurich, Switzerland, <sup>2</sup>Department of Earth Sciences, Utrecht University, Utrecht, The Netherlands, <sup>3</sup>Department of Earth and Planetary Science, Brown University, Providence, RI, USA, <sup>4</sup>ENS de Lyon, CNRS, Univ Lyon 1, UMR 5276 LGL-TPE, Lyon, France, <sup>5</sup>GNS Science, Lower Hutt, New Zealand, <sup>6</sup>ISMER—Institute of Marine Sciences, University of Quebec Rimouski, Rimouski, QC, Canada, <sup>7</sup>Collège de France, CEREGE, Aix-Marseille University, CNRS, IRD, INRAE, Aix-en-Provence, France, <sup>8</sup>Institute of Geosciences, Kiel University, Kiel, Germany,

<sup>9</sup>Now at Institute of Organic Biogeochemistry in Geo-Systems, RWTH Aachen University, Aachen, Germany,

<sup>10</sup>Department of Earth and Planetary Sciences, Harvard University, Cambridge, MA, USA, <sup>11</sup>Woods Hole Oceanographic Institution, Woods Hole, MA, USA, <sup>12</sup>Department of Earth, Geographic and Climate Sciences, University of Massachusetts Amherst, Amherst, MA, USA, <sup>13</sup>Key Laboratory of Marine Eco-Environmental Science and Technology, Marine Bioresource and Environment Research Center, The First Institute of Oceanography, Ministry of Natural Resources, Qingdao, China, <sup>14</sup>Department of Chemistry, University of York, York, UK, <sup>15</sup>Universidad Católica de la Santísima Concepción, Concepción, Chile, <sup>16</sup>MARUM, University of Bremen, Bremen, Germany, <sup>17</sup>Institut de Ciència i Tecnologia Ambientals, Universitat Autònoma de Barcelona (ICTA-UAB), Catalonia, Spain, <sup>18</sup>Department of Earth and Environmental Sciences, University of Manchester, Manchester, UK, <sup>19</sup>Antarctic Research Centre, Victoria University of Wellington, Wellington, New Zealand, <sup>20</sup>Leibniz Laboratory for Radiometric Dating and Isotope Research, Kiel University, Kiel, Germany, <sup>21</sup>Institute of Tibetan Plateau Research, Chinese Academy of Sciences, Beijing, China, <sup>22</sup>Alfred Wegener Institute, Helmholtz Centre for Polar and Marine Research, Bremerhaven, Germany, <sup>23</sup>Department of Chemistry, University of Wyoming, Laramie, WY, USA, <sup>24</sup>Netherlands Institute of Sea Research (NIOZ), 't Horntje, The Netherlands, <sup>25</sup>Sorbonne Université, CNRS, EPHE, PSL, UMR METIS, Paris, France, <sup>26</sup>State Key Laboratory of Marine Geology, Tongji University, Shanghai, China, <sup>27</sup>GFZ German Research Centre for Geosciences, Potsdam, Germany, <sup>28</sup>State Key Laboratory of Loess and Quaternary Geology, Institute of Earth Environment, Chinese Academy of Sciences, Xi'an, China, <sup>29</sup>University of Plymouth, Plymouth, UK, <sup>30</sup>Max Planck Institute for Chemistry, Mainz, Germany, <sup>31</sup>School of Chemistry, University of Bristol, Bristol, UK, <sup>32</sup>Now at Department of Earth Sciences, Utrecht University, Utrecht, The Netherlands, <sup>33</sup>Key Laboratory of Ecological and Environmental Change in Subtropical Zone, College of Geographic Science, Hunan Normal University, Changsha, China, <sup>34</sup>Department of Stratigraphy and Paleontology, University of Granada, Granada, Spain, <sup>35</sup>Frontiers Science Center for Deep Ocean Multispheres and Earth System, Key Laboratory of Marine Chemistry Theory and Technology, Ministry of Education, Institute for Advanced Ocean Studies, Ocean University of China, Qingdao, China, <sup>36</sup>Indian Institute of Science Education and Research (IISER) Kolkata, Mohanpur, India, <sup>37</sup>Department of Geology and Environmental Sciences, University of Pittsburgh, Pittsburgh, PA, USA, <sup>38</sup>Department of Geological Sciences, Stockholm University, Stockholm, Sweden, <sup>39</sup>Now at Swiss Federal Institute for Forest, Snow and Landscape Research WSL, Birmensdorf, Switzerland, <sup>40</sup>Department of Geology and Geophysics, University of Wyoming, Laramie, WY, USA, <sup>41</sup>Department of Geosciences, University of Arizona, Tucson, AZ, USA, <sup>42</sup>Department of Earth System Science, Hokkaido University, Sapporo, Japan, <sup>43</sup>School of Geography and Information Engineering, China University of Geosciences, Wuhan, China, <sup>44</sup>MOE Key Laboratory of Western China's Environmental Systems, Collaborative Innovation Centre for Arid Environments and Climate Change, Lanzhou University, Lanzhou, China

**Abstract** Ratios of glycerol dialkyl glycerol tetraethers (GDGT), which are membrane lipids of bacteria and archaea, are at the base of several paleoenvironmental proxies. They are frequently applied to soils as well as lake- and marine sediments to generate records of past temperature and soil pH. To derive meaningful environmental information from these reconstructions, high analytical reproducibility is required. Based on submitted results by 39 laboratories from across the world, which employ a diverse range of analytical and quantification methods, we explored the reproducibility of brGDGT-based proxies (MBT'<sub>5ME</sub>, IR, and #rings<sub>tetra</sub>) measured on four soil samples and four soil lipid extracts. Correct identification and integration of 5- and 6-methyl brGDGTs is a prerequisite for the robust calculation of proxy values, but this can be challenging as indicated by the large inter-laboratory variation. The exclusion of statistical outliers improves the reproducibility, where the remaining uncertainty translates into a temperature offset from median proxy values of 0.3–0.9°C and a pH offset of 0.05–0.3. There is no apparent systematic impact of the extraction method and sample preparation steps on the brGDGT ratios. Although reported GDGT concentrations are generally consistent within laboratories, they vary greatly between laboratories. This large variability in brGDGT quantification may relate to variations in ionization efficiency or specific mass spectrometer settings possibly impacting the response of brGDGTs masses relative to that of the internal standard used. While ratio values of GDGT are generally comparable, quantities can currently not be compared between laboratories.

## 1. Introduction

Glycerol dialkyl glycerol tetraethers (GDGTs) form the basis of several organic proxies used for the reconstruction of past environmental conditions. For example, archeal isoprenoid GDGTs (isoGDGTs) preserved in marine sediments are used as proxy for seawater temperature reconstructions, based on the degree of cyclization of these compounds, quantified in the TEX<sub>86</sub> lipid paleothermometer (Schouten et al., 2002). Similarly, the branched and isoprenoid tetraether (BIT) index, used to reconstruct soil-derived organic matter input to marine sediments (Hopmans et al., 2004), is based on the relative contribution of branched GDGTs (brGDGTs) produced by heterotrophic soil bacteria to crenarchaeol, an isoGDGT that is exclusively produced by Nitrososphaerota (formerly Crenarchaeota and Thaumarchaeota) (Sinninghe Damsté et al., 2002). Crenarchaeol is also used as a tracer for aerobic ammonium oxidation in (suboxic) terrestrial environments (i.e., Yang et al., 2019). In addition, the distribution of brGDGTs serves as a paleothermometer for terrestrial temperatures; it is based on their degree of methylation, which was found to increase with decreasing temperature in globally distributed surface soils (Weijers, Schouten, et al., 2007). This mechanism forms the basis of the MBT'<sub>5ME</sub> proxy (Equation 1), which only uses the brGDGTs with a methyl group on the fifth carbon position (5-methyl brGDGTs) in the alkyl chain (De Jonge, Hopmans, et al., 2014) in contrast to those with a methyl group on the sixth carbon position (i.e., 6-methyl brGDGTs) or other carbon atoms (Ding et al., 2016). Although different calibrations exist to translate MBT'<sub>5ME</sub> into temperatures for soils (Dearing Crampton-Flood et al., 2020; De Jonge, Hopmans, et al., 2014), peats (Naafs et al., 2017), and lakes (Martínez-Sosa et al., 2021), the temperature dependence of the MBT'<sub>5ME</sub> has been shown to be near-universal (Raberg et al., 2022). The application of this proxy to different sedimentary archives—such as river fan sediments that receive substantial contributions from land, loess-paleosol sequences, ancient peats/lignites, or lake sediments—has led to an ever-expanding collection of continental temperature records that span a wide range of timescales (e.g., Inglis et al., 2017; Lauretano et al., 2021; Lu et al., 2019; O'Connor et al., 2023; Peterse et al., 2011; Sinninghe Damsté et al., 2012; Weijers, Schefuß, et al., 2007). Furthermore, both the degree of cyclization of the alkyl chains (Weijers, Schouten, et al., 2007) and the abundance of 6-methyl brGDGTs relative to that of the 5-methyl brGDGTs, used in the CBT' ratio, are linked to pH in mineral soils (De Jonge, Hopmans, et al., 2014; Yang et al., 2015) and peats (Naafs et al., 2017). These differences in membrane structures can also be separately quantified using the #rings of tetra-, penta-, or hexamethylated brGDGTs (Sinninghe Damsté, 2016) or the isomer ratio (IR; De Jonge, Stadnitskaia, et al., 2014) for the relative abundance of 6-methyl brGDGT isomers. Notably, the existence of 6-methyl isomers, partially or fully co-eluting with their 5-methyl homologs using the original chromatographic method based on a single cyano column (Hopmans et al., 2004), was only recognized using improved chromatographic methods and after the isolation and structural identification of these compounds (Becker et al., 2013; De Jonge et al., 2013; Zech et al., 2012). Following the widespread presence of these compounds in a wide range of modern environments (e.g., De Jonge, Hopmans, et al., 2014), Hopmans et al. (2016) developed a liquid chromatography method that further improved

the separation of these isomers using two BEH HILIC UHPLC columns in tandem. This method of GDGT analysis is currently used by most organic geochemistry laboratories worldwide.

Analytical reproducibility, including both precision and accuracy, is crucial for the wide and comparable application of biomarker-based proxies to quantify key environmental parameters such as temperature in the geological past. A first study comparing the measurement and quantification of biomarkers between laboratories focused on alkenones in marine sediments (Rosell-Melé et al., 2001) that are linked to sea surface temperatures in their degree of unsaturation, quantified in the  $\text{U}^{\text{K}}_{37}$  index (Brassell et al., 1986; Prahl & Wakeham, 1987). This intercomparison study paved the way for studies comparing other temperature proxies developed by different disciplines, such as Mg/Ca measurements of planktonic foraminifera (Rosenthal et al., 2004) or carbonate clumped isotope measurements (Bernasconi et al., 2021), but also those based on biomarkers. Specifically, the  $\text{TEX}_{86}$  and the BIT indices have previously been assessed in two interlaboratory comparison studies (Schouten et al., 2009, 2013). The first round robin study was performed in 2008, when 15 laboratories analyzed the polar GDGT-containing fraction of two sediment extracts and submitted their results of  $\text{TEX}_{86}$  and BIT index values (Schouten et al., 2009). This study found that the repeatability, that is, the intralaboratory variation based on replicate runs of the same sample, of both proxies was small; whereas, the reproducibility, that is, the interlaboratory variation, could vary by up to 3–4°C for  $\text{TEX}_{86}$ -derived sea surface temperature (SST) estimates but was especially larger for the BIT index, which could be up to 0.4 on a scale of 0–1. The offset in the BIT index was attributed to the relatively large difference in molecular weight between the isoprenoidal GDGT crenarchaeol ( $m/z$  1,292) and the brGDGTs ( $m/z$ 's 1,022–1,050), and how they are detected by used mass spectrometers. Thus, the second round robin study from 2012 consisting of 35 participating laboratories included mixtures of isolated brGDGTs and crenarchaeol using known pre-weighed quantities in addition to homogenized and pre-extracted sediments (Schouten et al., 2013). The results from this second study showed an improved reproducibility of the  $\text{TEX}_{86}$  index compared with the first round robin study, translating to SST differences between 1.3 and 3.0°C. However, the reproducibility of BIT index values for the mixtures with known molar ratios of crenarchaeol and brGDGTs was again poor and reported BIT index values generally overestimated the molar-based values again pointing toward a different mass-spectrometric response between these two classes of GDGTs. This finding resulted in the recommendation to use calibrated standards to optimize comparability among laboratories.

So far, the reproducibility of the brGDGT-based  $\text{MBT}'_{\text{SME}}$ , IR, and #rings<sub>tetra</sub> proxies has never been assessed. Therefore, we conducted an anonymized round-robin study to specifically target brGDGT-based proxies. A total of 39 laboratories based in 15 countries worldwide participated in this study. The participating labs analyzed brGDGTs and crenarchaeol in four different homogenized soils and four polar fractions of soil extracts. Since the repeatability of GDGT analysis is generally monitored internally and reported in the literature as part of the methods, here we focus on the reproducibility of the proxy data. In addition to reporting the established indices, participating laboratories were asked to quantify crenarchaeol and brGDGTs using either an internal or external standard. This quantification allowed us to determine whether possible differences in the quantification of GDGTs result from interlaboratory variations in extraction or purification or from which mass-spectrometric system was used.

## 2. Methods

### 2.1. Study Setup

A general invitation to join the round robin study was sent to organic geochemistry laboratories worldwide and advertised online in September 2022. A total of 48 laboratories from 16 countries responded to this invitation. Sample sets were sent out in November 2022 to all participants. The laboratories received four centrifuge tubes containing homogenized soils labeled A–D and four 4-mL vials containing polar fractions of pre-extracted soils labeled E–H prepared at Utrecht University, The Netherlands, and ETH Zürich, Switzerland. The participating laboratories were asked to analyze the samples using their routine HPLC-MS method, following their local extraction and sample preparation protocols. In addition to the peak areas of the 15 brGDGTs that are generally integrated for calculating ratios that are applied as climate proxies, all laboratories were asked to report the peak areas for crenarchaeol to enable determination reproducibility of the BIT index reproducibility, which was low in the previous round robin studies that focused on isoGDGTs in marine samples (Schouten et al., 2009, 2013). Additionally, participating laboratories were asked to quantify crenarchaeol and the summed brGDGTs concentrations in the soil samples and soil extracts using either internal or external standards according to their protocols.

The participating laboratories did not know the origin of the soil samples and extracts to ensure an unbiased result. A dedicated email address was opened and monitored by a third person (T. Blattmann) to ensure anonymization of the results after submission. The results from 39 laboratories were received before the deadline and are reported here.

## 2.2. Sample Origin

*Soil A* “Canada, soil” was derived from the Black Creek Watershed on the Yukon coastal plain in the Western Canadian Arctic. The mean annual air temperature at the site is  $-10^{\circ}\text{C}$ . The soil was collected from the Bg horizon of the active layer in August 2018, and has a total organic carbon (TOC) content of 48% (Speetjens et al., 2022). The soil pH (measured in deionized  $\text{H}_2\text{O}$ , soil/water ratio of 1:2.5) was 4.9. The soil was freeze-dried and homogenized by hand using mortar and pestle, after which 100 g was extracted to yield Extract F. The remainder was divided into  $\sim 0.45$  g subsamples in 15-mL falcon tubes (Sample A).

*Soil B* “Switzerland, soil” was collected in the Pfynwald nature reserve in Valais, Switzerland, representing the A horizon (10–20 cm depth). The mean annual temperature at the site is  $10.7^{\circ}\text{C}$ . The soil was collected in 2019 and stored frozen before air drying and sieving using a 4 mm sieve. The pH of the soil was measured potentiometrically in 0.01 M  $\text{CaCl}_2$  with a solid-extractant ratio of 1:2, and reflects a slightly alkaline soil ( $\text{pH} = 7.3$ ) with a TOC content of 3.3%. After homogenization by mortar and pestle, a total of wt.%. 200 g was extracted to obtain Extract E. The remaining soil was divided into  $\sim 4$  g subsamples (Sample B).

*Soil C* “Rwanda, soil” was collected as part of the “TropSOC” project (DFG 387472333) in Mujabagiro ( $2.4645^{\circ}\text{S}$ ,  $29.10346^{\circ}\text{E}$ ), Rwanda, from an altitude of 1,908 m in a forest, representing a soil depth of 10–20 cm (NPL-1 C2). The mean annual temperature at the site is  $17.2^{\circ}\text{C}$  (TropSOC database; Doetterl et al., 2021). pH was measured in 1M KCl, reflecting an acidic soil ( $\text{pH} = 3.2$ ). The soil was sampled in 2018, air-dried, and stored at room temperature. After homogenization by mortar and pestle, approximately 200 g of soil was extracted to obtain Extract H. Subsamples ( $\sim 3.2$  g) of remaining soil were distributed as Sample C.

*Soil D* “Brazil, soil” was collected from a site in the Amazon Basin ( $49.4524^{\circ}\text{W}$ ,  $14.30296^{\circ}\text{S}$ ), Brazil, located within a Cerrado dry forest biome, and represents a dry forest topsoil (A horizon, 0–5 cm depth). The mean annual temperature at the site is  $26^{\circ}\text{C}$ , and the soil pH is 6.7 (Häggi et al., 2023). The soil was sampled in 2019, and transported at room temperature before freeze-drying and homogenization by mortar and pestle. Subsamples of  $\sim 3.0$  g were distributed as sample D.

*Extract E* “Switzerland, extract” is derived from Soil B. All extracts represent the same aliquot volume and thus brGDGT concentration.

*Extract F* “Canada, extract” is derived from Soil A. All extracts represent the same aliquot volume and thus brGDGT concentration.

*Extract G* “The Netherlands, extract” is obtained from a grassland soil (0–10 cm) at Utrecht Science Park, the campus where part of Utrecht University resides. The mean annual air temperature in Utrecht is  $10.5^{\circ}\text{C}$ . The soil has a TOC content of  $\sim 8$  wt.% and a pH ( $\text{H}_2\text{O}$ ) of 5.3. A large quantity of this soil was collected in 2017 to be used as a standard to monitor the performance of the HPLC-MS systems in the organic geochemistry laboratory at Utrecht University. A subsample ( $\sim 44$  g) of the freeze-dried and homogenized soil was used to generate Extract G for this study.

*Extract H* “Rwanda, extract” is derived from soil C. All extracts represent the same aliquot volume and thus brGDGT concentration.

## 2.3. Preparation of GDGT Fractions

All freeze-dried and homogenized soils were extracted at Utrecht University, where batches of 40–60 g, depending on the soil type, were Soxhlet extracted using a 15:2 mixture (v/v) of dichloromethane (DCM):methanol (MeOH) for 24 hr. Solvents were subsequently removed using rotary evaporation. 300–400 mg of total lipid extract per soil was fractionated using 60 g ( $23 \times 1.6$  cm column) of  $\text{Al}_2\text{O}_3$  as the stationary phase, eluting with four column-volumes of *n*-hexane:DCM (1:1) to obtain apolar fractions, followed by four column-volumes of DCM:MeOH (95:5) to yield the polar fractions containing the GDGTs. After rotary evaporation, the yields of the polar fractions were determined gravimetrically. Subsequently, a 1: 80 aliquot was taken to check for the

distribution and concentrations of the branched GDGTs following the HPLC-MS method used at Utrecht University. Based on these results, approximately 80 aliquots were prepared for each of the Extracts E–H, transferred to 4 mL vials, and dried overnight. Between the extracts E–H, the dry weight varied between 0.6 and 1.5 mg.

## 2.4. GDGT Proxy Calculations and Quantification

The following ratios and indices were used to quantify the relative abundances of the GDGTs based on the peak areas reported by each of the laboratories. Roman numerals refer to molecular structures (Figure S1 in Supporting Information S1) as in De Jonge, Hopmans, et al. (2014), where the branched GDGTs with a methylation on the 6-position are indicated with a prime symbol (').

$$\text{MBT}'_{5\text{ME}} = (\text{Ia} + \text{Ib} + \text{Ic})/(\text{Ia} + \text{Ib} + \text{Ic} + \text{IIa} + \text{IIb} + \text{IIc} + \text{IIIa}) \quad (1)$$

was used to quantify the degree of methylation of the 5-methyl branched GDGTs (De Jonge, Hopmans, et al., 2014).

$$\text{MBT}' = (\text{Ia} + \text{Ib} + \text{Ic})/(\text{Ia} + \text{Ib} + \text{Ic} + \text{IIa} + \text{IIa}' + \text{IIb} + \text{IIb}' + \text{IIc} + \text{IIc}' + \text{IIIa} + \text{IIIa}') \quad (2)$$

was used to quantify the degree of methylation of the summed 5-methyl and 6-methyl brGDGTs (Peterse et al., 2012) to determine whether offsets in the  $\text{MBT}'_{5\text{ME}}$  were caused by erroneous integration of 5- and 6-methyl brGDGTs.

$$\text{CBT}' = \log_{10}\left(\left(\text{Ic} + \text{IIa}' + \text{IIb}' + \text{IIc}' + \text{IIIa}' + \text{IIIb}' + \text{IIIc}'\right)/(\text{Ia} + \text{IIa} + \text{IIIa})\right) \quad (3)$$

was used to quantify the degree of cyclized tetramethylated 5-methyl and the relative abundance of 6-methyl branched GDGTs (De Jonge, Hopmans, et al., 2014). To further separate the influence of cyclization and relative abundance of 5- and 6-methyl isomers, the isomer ratio (IR) (De Jonge, Stadnitskaia, et al., 2014) and the #rings<sub>tetra</sub> (Sinninghe Damsté, 2016) were also calculated.

$$\text{IR} = \left(\text{IIa}' + \text{IIb}' + \text{IIc}' + \text{IIIa}' + \text{IIIb}' + \text{IIIc}'\right)/\left(\text{IIa} + \text{IIa}' + \text{IIb} + \text{IIb}' + \text{IIc} + \text{IIc}' + \text{IIIa} + \text{IIIa}' + \text{IIIb} + \text{IIIb}' + \text{IIIc} + \text{IIIc}'\right) \quad (4)$$

$$\#\text{rings}_{\text{tetra}} = (\text{Ib} + 2 \times \text{Ic})/(\text{Ia} + \text{Ib} + \text{Ic}) \quad (5)$$

Finally, the BIT index was calculated following Hopmans et al. (2004), rewritten to explicitly include the 6-methyl isomers (sensu De Jonge, Hopmans, et al., 2014):

$$\text{BIT index} = \left(\text{Ia} + \text{IIa} + \text{IIa}' + \text{IIIa} + \text{IIIa}'\right)/\left(\text{Ia} + \text{IIa} + \text{IIa}' + \text{IIIa} + \text{IIIa}' + \text{crenarchaeol}\right) \quad (6)$$

Quantities of crenarchaeol and GDGTs were reported by the participating laboratories in ng per g dry soil for Soils A–D, and ng per vial for Extracts E–H.

## 2.5. Data Handling and Statistical Analysis

### 2.5.1. Metadata

Information on the HPLC column used, HPLC solvent systems/gradients, phase type of separation, mass spectrometer (MS) type and method, as well as integration settings, was provided by the participating laboratories (Table S1, <http://hdl.handle.net/20.500.11850/666016>). Information on HPLC-MS type is not reported uniformly. In addition, for Soils A–D, extraction methods, solvent mixtures, further sample preparation and purification steps, and any standards used for quantification are reported. The metadata used in the discussion and figures are reported in Table 1. In Table 1 and the following discussion HPLC columns used were grouped into 8 classes based on similar column chemistry.

**Table 1**  
*Reported Metadata Used in the Discussion*

Lab number	HPLC column	HPLC gradient	Chromatography phase	MS type	Extraction	Column
1	2x Waters Acuity UHPLC BEH HILIC	Hex:IPA	Normal phase	Triple Quad	Ultrasonic	Alox
2	2x Waters Acuity UHPLC BEH HILIC	Hex:IPA	Normal phase	Triple Quad	Ultrasonic	Na <sub>2</sub> SO <sub>4</sub> , Alox
3	2x Waters Acuity UHPLC BEH HILIC	Hex:IPA	Normal phase	Triple Quad	ASE	Alox
7	2x Waters Acuity UHPLC BEH HILIC	Hex:IPA	Normal phase	Single quad	ASE	Alox
9	2x ThermoFischer Scientific, UHPLC silica, 1.7	Hex:IPA	Normal phase	Triple Quad	Microwave	SiO <sub>2</sub>
10	2x Waters Acuity UHPLC BEH HILIC	Hex:IPA	Normal phase	Single quad	ASE	Alox
11	2x Waters Acuity UHPLC BEH HILIC	Hex:IPA	Normal phase	Orbitrap	Microwave	Alox
14	2x Waters Acuity UHPLC BEH HILIC	Hex:IPA	Normal phase	Orbitrap	ASE	SiO <sub>2</sub>
15	2x ThermoFischer Scientific, UHPLC silica, 1.9	Hex:EtOAc	Normal phase	Triple Quad	Ultrasonic	SiO <sub>2</sub>
16	GL SCIENCES Inertsil SII—100A	Hex:IPA	Normal phase	Triple Quad	Ultrasonic	SiO <sub>2</sub>
17	2x Waters Acuity UHPLC BEH HILIC	Hex:IPA	Normal phase	Single quad	ASE	SiO <sub>2</sub>
18	2x Waters Acuity UHPLC BEH HILIC	Hex:IPA	Normal phase	Single quad	Ultrasonic	Activated Cu, Na <sub>2</sub> SO <sub>4</sub> , SiO <sub>2</sub>
19	2x Waters Acuity UHPLC BEH HILIC	Hex:IPA	Normal phase	Single quad	ASE	SiO <sub>2</sub>
20	2x Waters Acuity UHPLC BEH HILIC	Hex:IPA	Normal phase	Single quad	EDGE	Alox
21	2x Waters Acuity UHPLC BEH HILIC	Hex:IPA	Normal phase	Single quad	ASE	NH <sub>2</sub> column, SiO <sub>2</sub> , Alox
22	2x Waters Acuity UHPLC BEH HILIC	Hex:IPA	Normal phase	Single quad	Ultrasonic	None
24	2x Waters Acuity UHPLC BEH HILIC	Hex:IPA	Normal phase	Single quad	ASE	Alox
25	2x Waters Acuity UHPLC BEH HILIC	Hex:IPA	Normal phase	Triple Quadrupole/Ion Trap MS	Ultrasonic	None
26	2x Waters Acuity UHPLC BEH HILIC	Hex:IPA	Normal phase	Single quad	Microwave	SiO <sub>2</sub>
27	2x ThermoFischer Scientific, UHPLC silica, 1.9	Hex:EtOAc	Normal phase	Single quad	Ultrasonic	Alox
30	2x Waters Acuity UHPLC BEH HILIC	Hex:IPA	Normal phase	Orbitrap	Ultrasonic	Saponification, SiO <sub>2</sub>
31	2x Waters Acuity UHPLC BEH HILIC	Hex:IPA	Normal phase	Single quad	Microwave	SiO <sub>2</sub>
32	Agilent HILIC Plus column	Hex:IPA	Normal phase	Triple Quad	Ultrasonic	None
33	2x Waters Acuity UHPLC BEH HILIC	Hex:IPA	Normal phase	Single quad	Ultrasonic	Alox
34	2x Waters Acuity UHPLC BEH HILIC	Hex:IPA	Normal phase	Single quad	Microwave	Si-NH <sub>2</sub>
35	2x Waters Acuity UHPLC BEH HILIC	Hex:IPA	Normal phase	Triple Quad	Ultrasonic	SiO <sub>2</sub>
36	2x Waters Acuity UHPLC BEH HILIC	Hex:IPA	Normal phase	Single quad	Microwave	Alox
38	2x Waters Acuity UHPLC BEH HILIC	Hex:IPA	Normal phase	Single quad	ASE	SiO <sub>2</sub>

**Table 1**  
*Continued*

Lab number	HPLC column	HPLC gradient	Chromatography phase	MS type	Extraction	Column
39	2x Waters Acuity UHPLC BEH HILIC	Hex:IPA	Normal phase	Single quad	Microwave	Alox
40	2x Waters Acuity UHPLC BEH HILIC	Hex:IPA	Normal phase	Single quad	ASE	SiO <sub>2</sub>
41	2x Waters Acuity UHPLC BEH HILIC	Hex:IPA	Normal phase	Triple Quad	Ultrasonic	SiO <sub>2</sub>
42	2x ThermoFischer Scientific, UHPLC silica, 1.9	Hex:IPA	Normal phase	Triple Quad	Ultrasonic	SiO <sub>2</sub>
43	2x Waters Acuity UHPLC BEH HILIC	Hex:IPA	Normal phase	Ion trap	Microwave	SiO <sub>2</sub>
44	2x Waters Acuity UHPLC BEH HILIC	Hex:IPA	Normal phase	Triple Quad	Bligh Dyer	1/3 no treatment, 1/3 SiO <sub>2</sub> , 1/3 acid hydrolysis
45	2x Waters Acuity UHPLC BEH HILIC	Hex:IPA:CHCl <sub>3</sub>	Normal phase	Single quad	Ultrasonic	Saponification, SiO <sub>2</sub>
46	Phenomenex Luna CN column	Hex:IPA	Normal phase	Ion trap	ASE	Alox
47	ACE 2.5 UltraCore 2.5, SuperPhenylHexyl	MeOH:IPA:NH <sub>3</sub> sol.	Reverse phase	Orbitrap	Ultrasonic	Hydrolysis
48	2x Waters Acuity UHPLC BEH HILIC	Hex:IPA	Normal phase	Triple Quad	Flow Blending	SiO <sub>2</sub> and florisil column
49	2x Waters Acuity UHPLC BEH HILIC	Hex:IPA	Normal phase	Single quad	Bligh Dyer	Alox

*Note.* Extended metadata can be found in Table S1, <http://hdl.handle.net/20.500.11850/666016>.

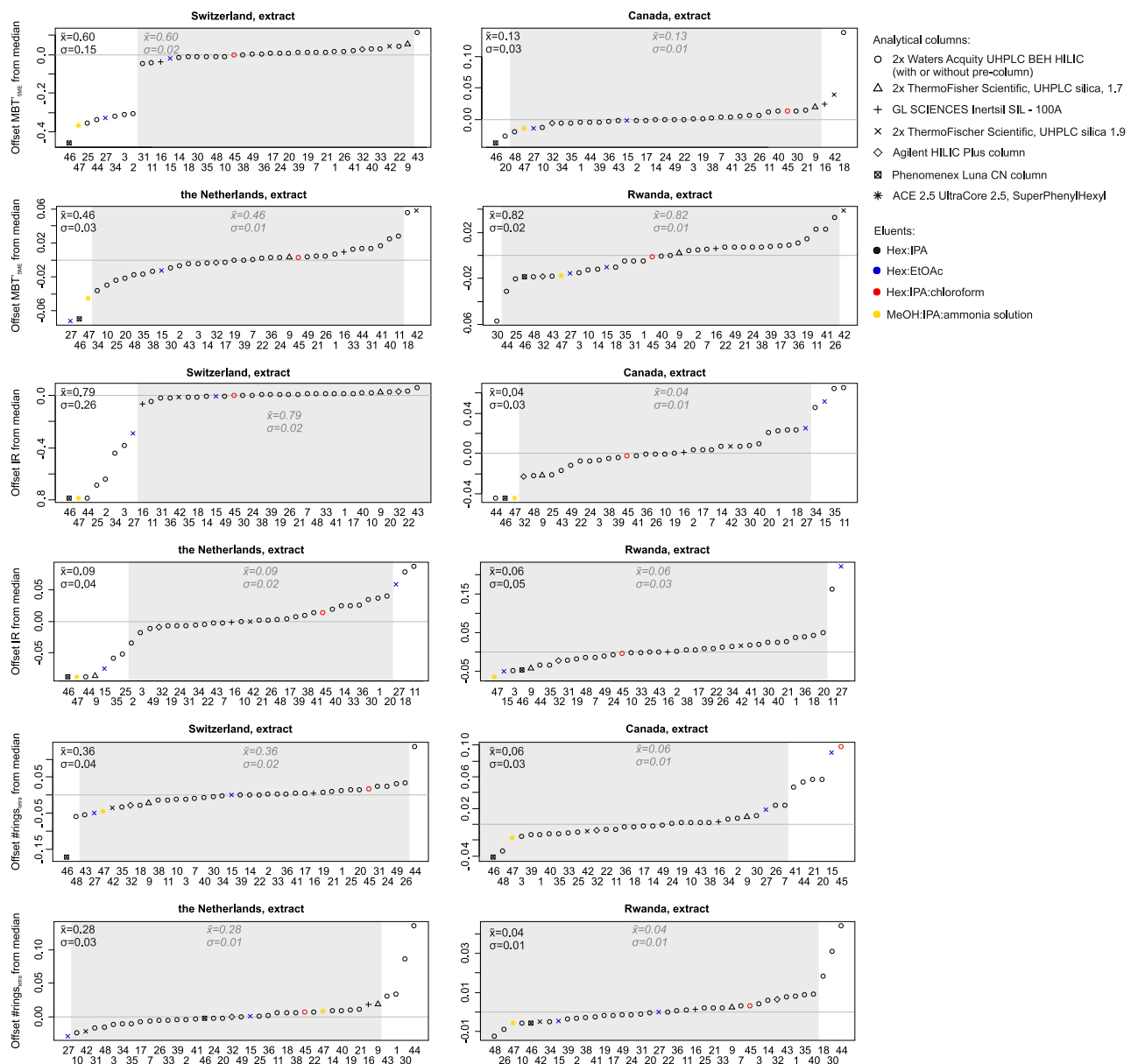


**Figure 1.** Offset of selected brGDGT ratio values ( $MBT'_{5ME}$ , IR, and  $\#rings_{tetra}$ ) from the median value per laboratory. Median value ( $\bar{x}$ ) and standard deviation ( $\sigma$ ) are reported with (black) and without (gray) outliers. The gray band indicates the range of ratio offset values after the exclusion of outliers. Symbols refer to liquid chromatography (LC) columns used, colors reflect different mobile phases.

### 2.5.2. Lipid Data

Participating laboratories provided lipid data as integrated peak areas and, when available, concentrations. No further quality control steps were performed by the two lead authors. This implies that we did not yet whether the reported areas comply with the detection limit reported by the individual laboratories. Ratios were calculated based on the areas reported; when no area is reported for a compound, the calculated fractional abundance value 0 is used for ratio calculation (Table S2, <http://hdl.handle.net/20.500.11850/666016>). Ratio values along with median and mean values, and standard deviations are calculated for each sample (A–H; Figure 1, Table 2). Samples with values larger or smaller than  $Q1 - 1.5 \times IQR$  (where  $Q$  = quartile,  $IQR$  = interquartile range), or larger than  $Q3 + 1.5 \times IQR$ , were considered outliers of the total data set (Tukey, 1977). Median values and standard deviations after exclusion of these outliers are reported in Figure 1 and Table S3, <http://hdl.handle.net/20.500.11850/666016>.

**Table 2**

Statistics of Selected GDGT Ratios per Sample ( $MBT'_{SME}$ ,  $MBT'$ , IR, CBT; #Ringstetra and BIT (Equations 1–6)). Specifically Median and Mean Value, As Well As the Standard Deviation (Stdev)

Sample	Sample name	$MBT'_{SME}$			$MBT'$			IR			CBT'			#Ringstetra			BIT		
		Median	Mean	Stdev	Median	Mean	Stdev	Median	Mean	Stdev	Median	Mean	Stdev	Median	Mean	Stdev	Median	Mean	Stdev
A	Canada, soil	0.129	0.163	0.151	0.123	0.155	0.151	0.042	0.069	0.107	-1.411	-1.362	0.423	0.061	0.071	0.041	1.000	0.999	0.002
B	Switzerland, soil	0.593	0.538	0.137	0.241	0.239	0.047	0.789	0.677	0.248	0.314	0.179	0.469	0.362	0.351	0.041	0.984	0.980	0.012
C	Rwanda, soil	0.820	0.800	0.117	0.805	0.782	0.113	0.066	0.102	0.137	-1.606	-1.541	0.302	0.047	0.060	0.054	0.991	0.990	0.007
D	Brazil, soil	0.943	0.914	0.056	0.815	0.811	0.021	0.723	0.590	0.267	-0.630	0.287	0.274	0.274	0.274	0.045	0.967	0.967	0.019
E	Switzerland, extract	0.597	0.533	0.149	0.241	0.237	0.027	0.786	0.666	0.262	0.321	0.09	0.615	0.36	0.354	0.042	0.983	0.982	0.01
F	Canada, extract	0.13	0.134	0.026	0.126	0.129	0.024	0.044	0.047	0.026	-1.362	-1.35	0.189	0.062	0.07	0.03	1.000	0.999	0.003
G	The Netherlands, extract	0.456	0.453	0.026	0.434	0.431	0.024	0.089	0.084	0.043	-1.038	-1.067	0.190	0.282	0.287	0.029	0.984	0.984	0.009
H	Rwanda, extract	0.824	0.822	0.018	0.813	0.811	0.020	0.064	0.072	0.051	-1.658	-1.657	0.192	0.044	0.046	0.010	0.994	0.994	0.003

Note. The same summary data after removal of outliers can be found in Table S2, <http://hdl.handle.net/20.500.11850/666016>.

To determine the impact of selecting 5-methyl and 6-methyl brGDGTs on the  $MBT'_{SME}$  and IR, we compared  $MBT'$  with  $MBT'_{SME}$  values, plotted against IR values (Figure 2). To determine the impact of extraction and laboratory processing on GDGT ratios, the offset in ratio values ( $MBT'_{SME}$ , IR, #ringstetra) between soil-extract pairs (i.e., Sample A and Extract F, B and E, C and H) were calculated for each laboratory (Figure 3). An initial check of the concentration data revealed unrealistic values for the Soil samples (A–D) of one laboratory (3), with 115–1,800 times higher crenarchaeol or brGDGT concentrations reported. For the concentrations of the Extracts (E–H), three laboratories reported unrealistic values (2, 3, 42, for isoGDGT) and brGDGT concentrations (with up to 680 times higher GDGT concentration reported). These concentration offsets are probably due to an error reporting units, for instance, pg instead of ng, or reporting the concentration per ng extract, instead of the full extract. Although the calculation of concentrations is clearly still non-trivial, these offsets cannot be explained by differences in the analysis of GDGTs. Therefore, while all concentration values are reported in Table S2, <http://hdl.handle.net/20.500.11850/666016>, the data from these few laboratories were excluded from further concentration analyses in this manuscript. In addition, concentrations that were reported to be 0 were excluded from the discussion. Concentration outliers were identified analogous to the ratios, that is, those values that are larger or smaller than  $Q1 - 1.5 \times IQR$ , or larger than  $Q3 + 1.5 \times IQR$  (Figure 4). As the range in concentration values excluding the outliers was still substantial (Table 3), scatterplots were used to compare the impact of MS type on crenarchaeol and brGDGT ionization in the Extracts (Figure 5), as well as the impact of extraction method on the concentration in soils (Figure 6).

### 3. Results and Discussion

The results from 39 laboratories were received and are reported as ratios, that is,  $MBT'_{SME}$ , IR, #ringstetra, to assess (a) the impact of chromatography (LC column and mobile phase), presented in Figure 1; and (b) the impact of the extraction method and workup procedures, presented in Figure 3. An overview of all ratio values can be found in Table S2, <http://hdl.handle.net/20.500.11850/666016>, and a summary of the statistics is presented in Table 2 and Table S3, <http://hdl.handle.net/20.500.11850/666016>.

#### 3.1. Influence of HPLC Column and Mobile Phase on GDGT Proxies in Extracts

The HPLC methods used by the participating laboratories were overall comparable, yet differed in several aspects, summarized in Table 1. In short, most labs ( $n = 30$ ) use two Waters Acuity UHPLC BEH HILIC Silica columns (with or without pre-column) in tandem as the stationary phase, and *n*-hexane:iso-propanol (IPA) as the mobile phase, following the method developed by Hopmans et al. (2016), except for one lab that uses hexane:IPA:chloroform as the mobile phase. Other columns used are Waters Acuity UHPLC BEH HILIC Amide columns ( $n = 1$ ), ThermoFisher Scientific UHPLC Silica (1.7  $\mu$ m,  $n = 1$ , 1.9  $\mu$ m,  $n = 3$ ), GL SCIENCES Inertsil SIL—100A ( $n = 1$ ), Agilent HILIC Plus ( $n = 1$ ), Phenomenex Luna CN ( $n = 1$ ), and ACE UltraCore 2.5 Super PhenylHexyl ( $n = 1$ ). Two of the three laboratories that use ThermoFisher Scientific UHPLC Silica 1.9  $\mu$ m columns use *n*-hexane:ethyl acetate (EtOAc) as mobile phase, and the lab using an ACE UltraCore 2.5 Super

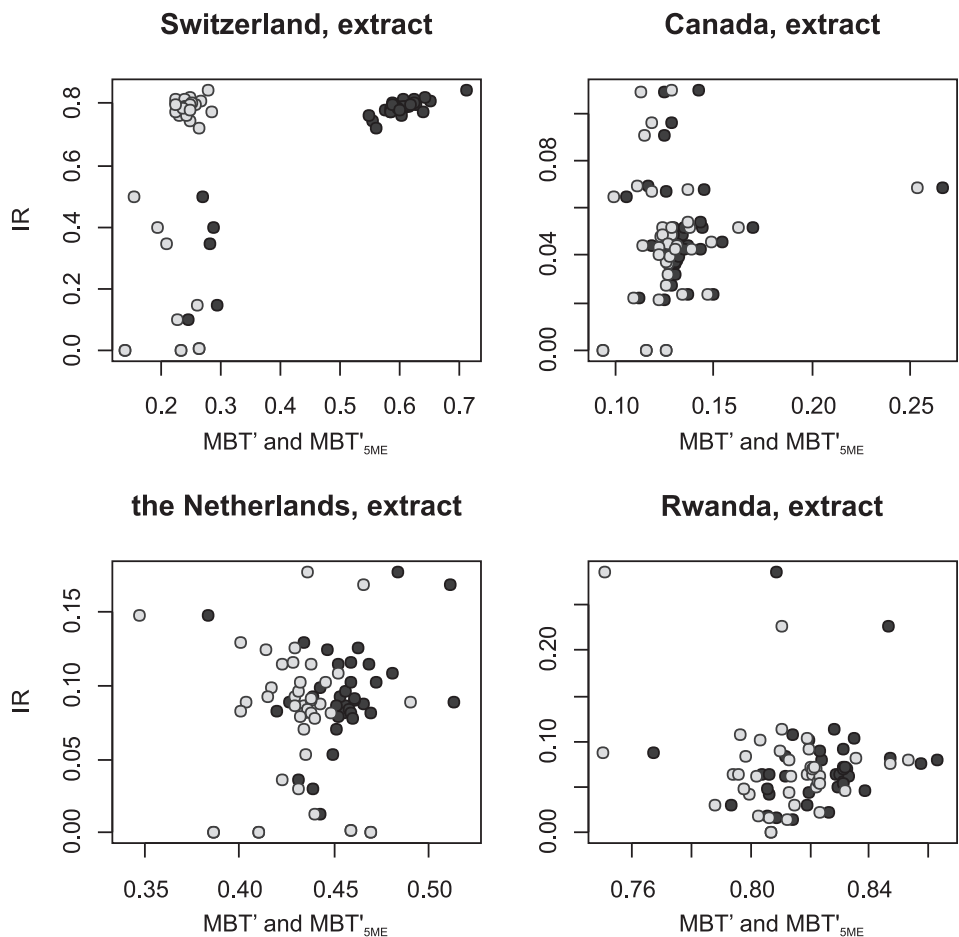


**Figure 2.** Scatterplot of the individual laboratory IR versus MBT' (gray) and MBT'5ME (black) values.

PhenylHexyl column uses a MeOH:IPA:ammonia solution and is the only participating laboratory that uses reverse phase chromatography as opposed to normal phase used by all other laboratories.

The polar fractions, containing GDGTs (Extract E–H), were provided to all participating laboratories to assess the potential influences of different HPLC columns and settings on GDGT proxies, independent of extraction and

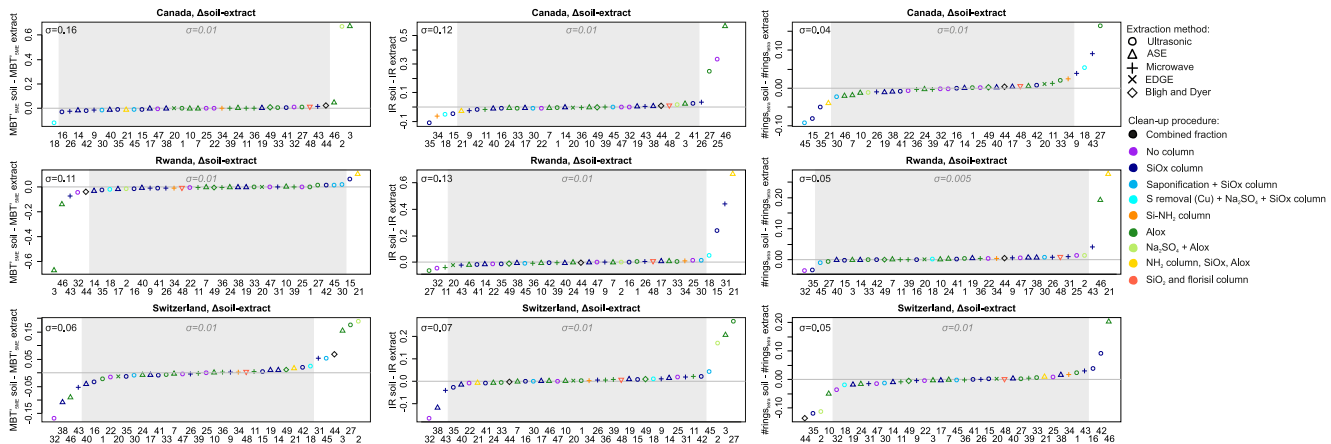


**Figure 3.** Offset of selected brGDGT ratio values (MBT'5ME, IR, and #rings<sub>tetra</sub>) of samples provided as Soil and as Extract per laboratory. Standard deviations ( $\sigma$ ) are reported with (black) and without (gray) outliers. The gray band indicates the range of values after the exclusion of outliers. Symbols refer to extraction methods and colors refer to subsequent processing steps used by the laboratories.

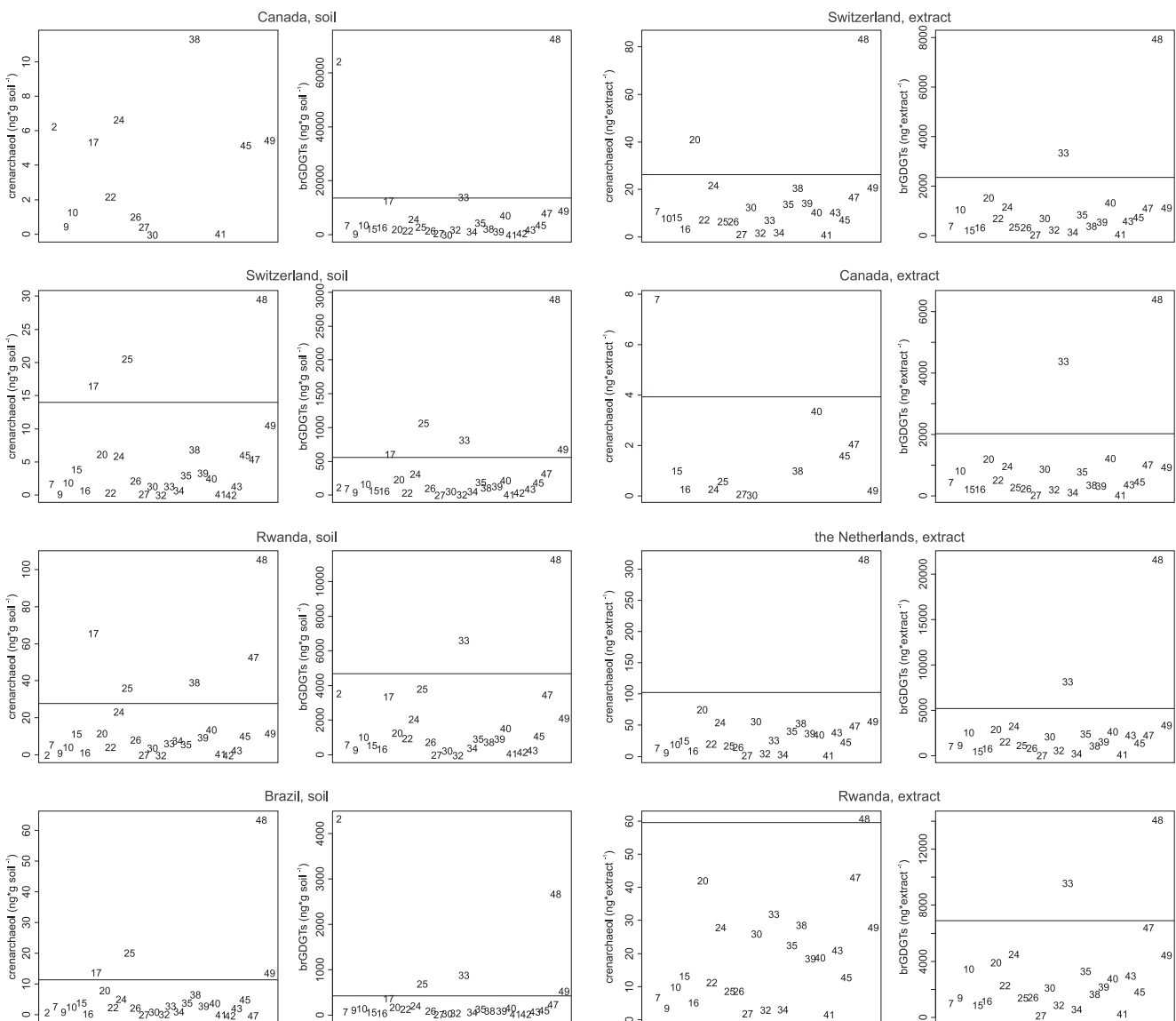


**Figure 4.** Concentrations of crenarchaeol and summed brGDGTs for all Soils and Extracts analyzed indicated by lab numbers. The upper limit of the interquartile range (IQR) is indicated by a horizontal line. Lower IQR limits are always below 0. When no horizontal line is plotted, all samples fall within the IQR.

separation techniques. The reported  $\text{MBT}'_{\text{SME}}$  values have a reasonably Gaussian distribution for most Extracts (Figure 1). However, the values for Extract E (Switzerland) are characterized by a  $\sim 0.25$ -unit jump caused by eight laboratories (2, 3, 25, 27, 34, 44, 46, 47) that reported substantially lower-than-average  $\text{MBT}'_{\text{SME}}$  values (Figure 1). The reproducibility for this extract is low ( $\sigma = 0.15$ ) compared with the other extracts, which all have a reproducibility  $< 0.03$  (Figure 1). When translated into temperatures, this would result in an offset of  $7.8^\circ\text{C}$ . Five laboratories reported  $\text{MBT}'_{\text{SME}}$  values that were defined as outliers for more than one extract (18, 27, 42, 46, 47). Four of these labs followed HPLC methods that deviate from Hopmans et al. (2016), and used a different mobile phase (MeOH:IPA:ammonia solution or hexane:EtOAC), different columns (ThermoFisher Scientific UHPLC Silica 1.9  $\mu\text{m}$  or Phenomenex Luna CN), or ran a reverse phase method with different mobile and stationary phases. Other laboratories ( $n = 5$ ), however, that used similar alternative normal phase methods produced  $\text{MBT}'_{\text{SME}}$  index values that were not marked as outliers. Similarly, seven outliers were from laboratories that followed standard methods. This suggests that outliers are more likely derived from instrument-specific settings rather than related to the different mobile and stationary phases used.

**Table 3**

Summary Statistics of the Reported Concentrations (Summed Concentration of brGDGTs or Concentration of Crenarchaeol) After Exclusion of Outliers

Sample	Sample name	$\Sigma$ brGDGT concentration ( $\text{ng} * \text{gsoil}^{-1}$ or $\text{ng} * \text{extract}^{-1}$ )		Cren concentration ( $\text{ng} * \text{gsoil}^{-1}$ or $\text{ng} * \text{extract}^{-1}$ )	
		Mean	Stdev	Mean	Stdev
A	Canada, soil	3,448.95	3,111.44	3.54	3.48
B	Switzerland, soil	125.80	92.12	2.83	2.77
C	Rwanda, soil	1,207.30	1,176.35	6.52	5.81
D	Brazil, soil	101.28	82.33	2.68	2.20
E	Switzerland, extract	666.39	433.81	10.02	6.33
F	Canada, extract	558.33	379.68	0.98	1.03
G	The Netherlands, extract	1,657.03	1,007.35	29.59	20.86
H	Rwanda, extract	2,270.99	1,561.60	16.44	12.43

Note. Specifically, mean values and standard deviation (stdev) are reported.

The degree of cyclization of brGDGTs is relatively insensitive in soils with  $\text{pH} < 5$  (De Jonge, Hopmans, et al., 2014), which is reflected by the similarly low  $\# \text{rings}_{\text{tetra}}$  values of 0.04 and 0.06 for Extracts H and F, although the measured pH of the soils used to generate these extracts differs by 1.7 units. Extract G has a  $\# \text{rings}_{\text{tetra}}$  value of 0.28 and Extract E -from the highest pH soil-has a  $\# \text{rings}_{\text{tetra}}$  value of 0.36. The reproducibility was relatively high ( $\sigma < 0.04$ ) for all Extracts, indicating that the detection and identification of brGDGTs with cyclopentane moieties are generally consistent between laboratories (Figure 1). The outliers, which mostly overestimate the degree of cyclization of brGDGTs in these extracts, do not differ in HPLC methodology. One laboratory (44) that reports deviating values for all extracts follows the standard method of Hopmans et al. (2016).

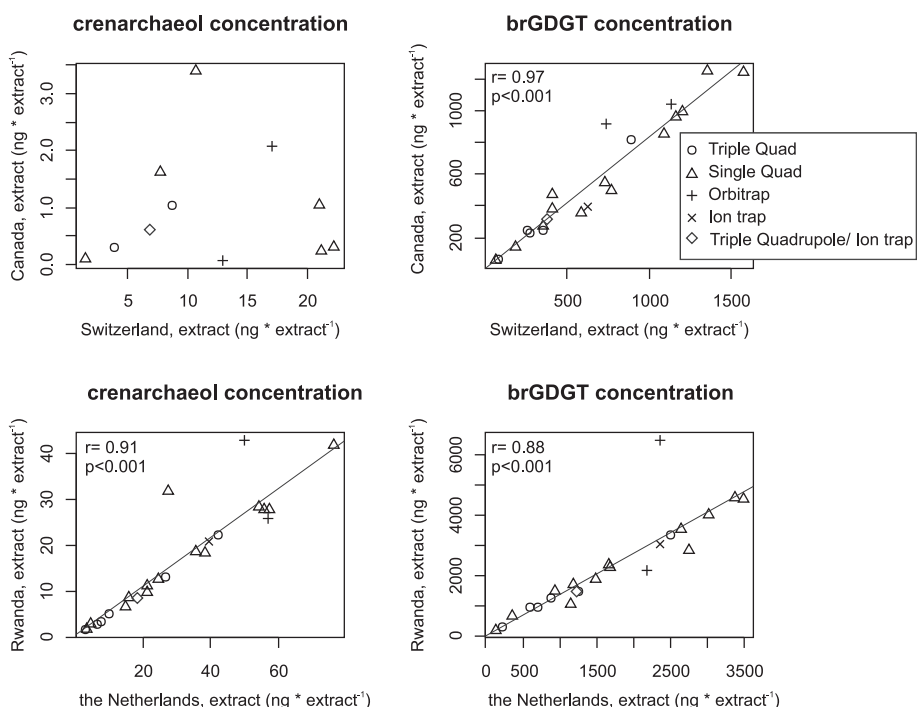


**Figure 5.** Scatterplots of the concentrations of crenarchaeol (left) or summed brGDGTs (right), comparing two extracts in each panel. Correlation line, Pearson  $r$ -value and  $p$ -value are reported for significant correlations ( $p < 0.05$ ). Symbols refer to the type of mass-spectrometer.

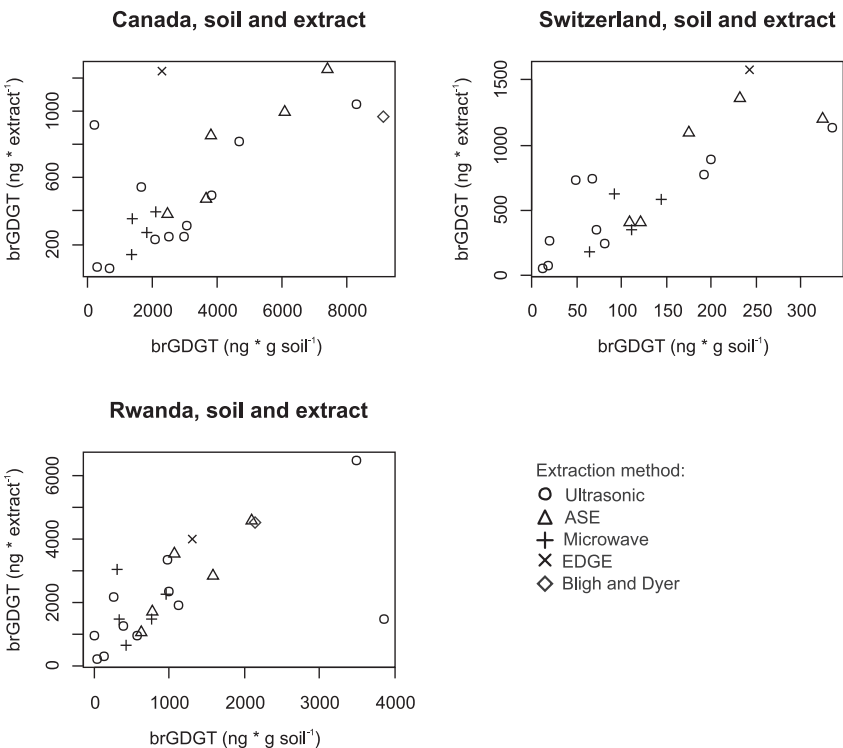


**Figure 6.** Comparison of reported concentrations of summed brGDGTs between samples that were provided as Soils and those provided as Extracts. Note that a direct comparison is not possible as a different normalization is used for Extracts and Soils (x and y-axes). Symbols refer to extraction methods.

The IR showed values between 0.04 and 0.09 for the three acidic soil extracts with a reproducibility  $\sigma < 0.05$ . These low IR values result from the low contributions of 6-methyl brGDGTs in these soils. Analogous to the  $\#_{\text{rings}_{\text{tetra}}}$ , the similar IR values for the three acidic soils, despite the  $>2$  pH range that they cover, fits with the trend in the global surface soil data set (including both mineral soils and peats) used by Dearing Crampton-Flood et al. (2020); IR reaches 0 at pH values of  $\sim 4$ , indicating reduced sensitivity of the IR at the lower end of the pH range present in global soils. The alkaline soil from Switzerland (Extract E) had an IR of 0.79, reflecting the larger contribution of 6-methyl brGDGTs in this soil. However, the reproducibility for this extract was very low ( $\sigma = 0.26$ ). This is caused by much lower IR values, up to 0.6 difference from the median value, reported by the same eight laboratories that also reported the lower-than-average  $\text{MBT}'_{\text{SME}}$  values for this extract. This suggests that the offset in both ratios may stem from problems with the detection, separation, and/or identification of the 5- and 6-methyl brGDGT isomers. However, there are also laboratories that consistently report higher-than-median IR values for the three acidic soils (Rwanda, Canada, The Netherlands) but are not flagged as outliers for the  $\text{MBT}'_{\text{SME}}$  of these same extracts.

### 3.2. Influence of Peak Identification on GDGT Proxies in Extracts

To assess the influence of peak identification as a source of deviation on GDGT proxy values, we compared  $\text{MBT}'_{\text{SME}}$  index values, based on just the 5-methyl brGDGTs, with those of the  $\text{MBT}'$ , which includes both 5- and 6-methyl brGDGTs (Figure 2). The inclusion of 6-methyl isomers per definition results in lower values for the  $\text{MBT}'$  compared to the  $\text{MBT}'_{\text{SME}}$  (Figure 2). The highest offsets are expected for soils with large contributions of 6-methyl brGDGTs, that is, with a high soil pH. Indeed, the most pronounced difference between these indices is in Extract E (Switzerland) with a pH of 7.3. Here,  $\text{MBT}'$  values are up to 0.43 lower than  $\text{MBT}'_{\text{SME}}$  values for laboratories that also report high IR values. The offset between  $\text{MBT}'$  and  $\text{MBT}'_{\text{SME}}$  is much smaller ( $<0.12$ ) for the eight laboratories that had outliers for the  $\text{MBT}'_{\text{SME}}$  and IR in Section 3.1 (Figure 1). We postulate that these laboratories may have identified the 6-methyl brGDGT peaks as those of the 5-methyl brGDGTs in the chromatogram. This misidentification would result in a relative underestimation of the IR as well as the  $\text{MBT}'_{\text{SME}}$ . Conversely, the two outliers for the IR in Extract H (Rwanda) are linked to the largest offsets between  $\text{MBT}'$  and

MBT'<sub>5ME</sub> (Figure 2). In this case, the identification of (part of) the 5-methyl brGDGT peaks as belonging to the 6-methyl isomers may have resulted in a relative overestimation of IR and MBT'<sub>5ME</sub>. In addition to misidentification, chromatographic issues resulting in reduced separation of 5- and 6-methyl isomers may contribute to the offsets observed here. However, the laboratories that report outlier values are not characterized by a common deviating HPLC method, suggesting that offsets are again introduced by lab-specific approaches to peak integration and/or instrument settings rather than by the use of different mobile or stationary phases.

### 3.3. Influence of Sample Workup Procedure on GDGT Proxies in Soils

The sample workup procedures of the participating laboratories differed substantially; the most commonly applied method was ultrasonic extraction ( $n = 16$ ), followed by Accelerated Solvent Extraction (ASE) ( $n = 11$ ), microwave assisted extraction ( $n = 8$ ), Bligh and Dyer extraction ( $n = 1$ ), EDGE automated solvent extraction ( $n = 1$ ), and flow blending ( $n = 1$ ). The vast majority of laboratories used a 9:1 mixture of DCM:MeOH for lipid extraction ( $n = 35$ ), except for three laboratories that additionally used a buffer (phosphate and/or trichloroacetic acid) and one lab that used DCM:MeOH:hexane. The approaches used for further processing of the obtained lipid extract and separation into different fractions were very diverse, and consisted of no further treatment, hydrolysis, treatment with activated Cu, passing over a Na<sub>2</sub>SO<sub>4</sub> column, or column separation using Al<sub>2</sub>O<sub>3</sub>, SiO<sub>2</sub>, Si-NH<sub>2</sub>, or Florisil (Table S1, <http://hdl.handle.net/20.500.11850/666016>).

Evaluating the offsets between proxy values calculated based on brGDGTs in soils and matching extracts highlights that all extraction and separation methods used are able to successfully extract and purify brGDGTs. Taking the example of the soil-extract pair from Switzerland (Sample B and Extract E), some of the laboratories with offset MBT'<sub>5ME</sub> and/or IR values for the Extracts (attributed to integration errors; see Section 3.1) report more accurate values for MBT'<sub>5ME</sub> and IR in soils that they extracted themselves (lab 2, 3, 27, 44). This suggests that if the offsets were indeed introduced by integration errors, these errors were not made consistently. By comparison, other laboratories report offset values for both the Samples and Extracts (labs 25, 34, 46, 47). The exclusion of eight laboratories (2, 3, 25, 27, 34, 44, 46, 47), where integration issues may have caused the offset between extracts and soils highlights small offsets that can be linked to extraction and clean-up procedures. Concerning extraction methods, of the 15 laboratories whose offsets represent an outlier (Figure 3), three employ ASE extraction, five employ microwave extraction, and seven employ ultrasonic extraction, representing 27%, 63% and 43% of the laboratories that use these respective extraction methods. However, of those laboratories that show offsets more often (for instance more than three occurrences [Figure 3: maximum occurrence of offsets = 9]), five out of seven laboratories use ultrasonic extraction. This offset might be caused in part by the fact that Soxhlet extraction, used to prepare the extracts, and ultrasonic extraction are performed at different temperatures, and potentially extract a slightly different pool of brGDGTs. However, a large fraction of laboratories that use ultrasonic extraction are clearly able to extract brGDGTs from the soil Samples (A–D) in a distribution that is comparable to that in the provided Extracts (E–H). Variability in the wavelength frequency used for sonication can potentially be the cause of this discrepancy. All in all, the impact of post-extraction clean-up steps seems minor compared to the extraction method, and these observations are not statistically meaningful as some treatment protocols are only used once. For instance, the only laboratory that uses an NH<sub>2</sub> column after ASE extraction (lab 21) produces a pronounced offset brGDGT distribution only in the Rwandan soil. In addition, the only laboratory that uses activated Cu after ultrasonic extraction reported offset values for the soils from Canada and Rwanda (lab 18). Similarly, the separation of commonly used silica or Al<sub>2</sub>O<sub>3</sub> columns can result in either accurate or offset GDGT distributions. Therefore, the diverse approaches used by the 39 participating laboratories all seem to be mostly valid.

### 3.4. Quantification of GDGTs

Of the 39 labs that submitted data, 30 used standards to enable quantification of GDGTs. The synthetic C<sub>46</sub> glycerol trialkyl glycerol tetraether (GTGT) is used as an internal standard by 28 of these laboratories, while one laboratory (47) uses an H-shaped tetraester as internal standard. Finally, one laboratory (48) uses archeol as an external standard for quantification. Due to the large differences in GDGT abundances, data from three laboratories that reported unrealistically high values for the provided extracts have been excluded from further analyses (see Section 2.5). Still, range differences in the absolute GDGT concentrations, up to orders of magnitude, are reported (Figure 4). The laboratory that uses an external standard for quantification nearly consistently reports the highest GDGT abundances. Still, several other laboratories that reported two or more outlier abundances (2,

17, 25, 33, 49) all used C<sub>46</sub> GTGT as an internal standard. Hence, the type of internal standard does not explain the large range in absolute GDGT abundances, yet the use of an external standard seems to introduce a large deviation in the quantification, albeit based on the data of one laboratory only.

Crenarchaeol or total brGDGT concentrations compared between extracts were strongly correlated (Figure 5). This means that laboratories are consistent in their quantification, that is, laboratories that measured high GDGT concentrations in one Extract generally also measured high concentrations in all extracts and vice versa. When evaluating the impact of mass spectrometry methods, the use of orbitrap mass spectrometry can result in offset quantifications between samples (Figure 5). However, this is based on the performance of only two laboratories, one of which uses an external standard, and the unique impact of the orbitrap mass spectrometry on quantification cannot be constrained.

Instead, we propose that the large range in GDGT abundances reported per Extract may be introduced by instrument-specific settings, such as mass selection values, tuning settings, APCI settings and MS type, which may affect, for example, the ionization efficiency and detection of different GDGTs. For individual instruments, changes in the relative response factor between the internal standard and crenarchaeol with time have previously been attributed to instrument drift and tuning events (Huguet et al., 2006). Instrument specific settings have also been invoked to explain large offsets in BIT index values in a previous round-robin study focusing on isoGDGTs, where it was assumed that the relative response of crenarchaeol (or isoGDGTs as a group) and brGDGTs differed among MS systems (Schouten et al., 2013). Specifically, Davtian et al. (2018) showed that the impact of using approximate or unstable mass selection *m/z* values using SIM on calculated BIT index values amounts up to 0.1 unit. In this round robin, different response factors of the internal standard can impact quantification. Its impact on the BIT index is difficult to observe as the soils that were selected for this round robin study are all dominated by brGDGTs, with BIT index values of Soils A-C close to 1.00, whereas only Soil D (Brazil) shows some scatter and a range (0.91–1.00; Table S2, <http://hdl.handle.net/20.500.11850/666016>).

Finally, we assessed the consistency of quantification between GDGTs in Extracts and Soils based on three sets of soil-extract pairs, that is, lipid extracts generated by us and the matching soil extracts prepared by the participating laboratories: Soil A and Extract F (Canada), Soil A and Extract F (Canada), Soil B and Extract H (Rwanda), Soil AC and Extract E (Switzerland). There is a general correlation between the GDGT abundances in Extracts and Soils (Figure 6), indicating consistent quantification within laboratories. Given this, and the knowledge that Soils and Extracts are analyzed on the same instrument with the same settings, offsets from the general dependency are likely introduced during sample extraction and workup, for instance incomplete extraction or sample loss, or adding inaccurate amounts of internal standard. Different extraction methods do not show different results (Figure 6), suggesting that all perform equally well. Consequently, the preparation of extract aliquots is the final remaining source of uncertainty.

In general, the large range in quantified values provides an important indication that combining quantitative data sets from different laboratories requires a more rigorous approach and serious evaluation of quantification methods, for example, by exchanging sample material and analyzing the same samples in multiple laboratories.

#### 4. Conclusions and Recommendations

Our round-robin study based on four soils and the polar lipid fractions of four soil extracts showed good reproducibility of brGDGT-based proxies among the 39 participating laboratories, but also highlights several pitfalls. The observed offsets in proxy values are not related to specific LC-MS methods (e.g., stationary, mobile phase or mass spectrometer type). Similarly, offsets in proxy values between soils and matching extracts that are introduced during sample workup are not related to differences in workup procedure (e.g., extraction method, small column chromatography). Instead, some of the observed outliers in MBT'<sub>SME</sub> values can be explained by misidentification of 5- and 6-methyl brGDGTs and/or errors in peak integration, as the laboratories with offset MBT'<sub>SME</sub> values also have offset IR values. This is possibly caused by chromatography that separates brGDGTs insufficiently or human error when selecting peaks of 5-methyl and 6-methyl brGDGTs. We have included example chromatograms with integration from a laboratory that plots close to median values in all instances for comparison and future reference (Figure S2 in Supporting Information S1). Problems with selecting 5- and 6-methyl brGDGTs can happen more readily with samples that are dominated by either isomer set or where additional peaks are observed in the *m/z* 1,050 and 1,036 traces. For these samples, comparison of retention times

(potentially using aligning of well-defined brGDGT peaks to correct for retention time shift) with an internal standard that contains both isomer sets is strongly suggested.

The large spread in GDGT concentrations reported by the laboratories makes comparison of GDGT concentrations between laboratories challenging, although quantification within laboratories was generally consistent. Hence, accurate quantification of GDGTs remains the largest challenge in further improving the reproducibility of brGDGT analysis. As a first step to ensure comparable quantifications, errors in preparation of the internal standard from dry powder, adding known amounts of internal standard to the sample and finally calculation of the GDGT quantities need to be evaluated within laboratories. To ensure correct calculation of ratio values and quantities, we suggest that all laboratories shall use a standard mixture that includes all 15 brGDGTs as well as an internal ( $C_{46}$  GTGT) standard to assess the performance of their instrument, including both the response factor, consistency of GDGT-based proxy values as well as compound quantification. Ideally, the community will introduce a “reference sample”—a standard mixture with established proxy values that can be used as a benchmark in laboratories worldwide, as is usual procedure used to standardize isotope studies, for example, NSB-18 for carbonates. A rigorous approach to quantification would require the development of a reasonable structural brGDGT analog that can be used in individual laboratories to determine and monitor the instrument-specific response factor of brGDGTs.

## Data Availability Statement

The data used in this manuscript is presented in Supporting Information, where Table S1 includes the extended metadata and Table S2 includes the raw GDGT data submitted by the laboratories. In addition, these tables are hosted and accessible on the online repository “ETH Zurich research collection,” <http://hdl.handle.net/20.500.11850/666016>, under the doi: [10.3929/ethz-b-000666016](https://doi.org/10.3929/ethz-b-000666016). Following the set-up of this study, laboratories remain anonymous in the metadata table.

## Acknowledgments

The authors thank two reviewers, Sarah Feakins and Yunping Xu, for their constructive comments. In addition, we would like to thank Jorien Vonk (VU, The Netherlands) for providing Soil A from Canada, Frank Hagedorn (WSL, Switzerland) for Soil B from Switzerland, Sebastian Dörrerl (ETH, Switzerland) for Soil C from Rwanda, and Christoph Häggi (ETH, Switzerland) for Soil D from Brazil. Adele Blatter (ETH, Switzerland) has helped with the preparation of soil samples. This study received funding from NWO-Vidi Grant (192.074) awarded to FP and PRIMA (PROOP2\_179783) and SNSF Starting Grant (TMSGI2\_211319) grants from SNSF to CDJ. AS thanks the European Research Council for funding Consolidator Grant 771497 under Horizon 2020 program. SN, BD and TA thank GNS Science and Victoria University of Wellington for their ongoing support of the GNS/VUW Organic Geochemistry Laboratory, and the New Zealand Ministry of Business, Innovation and Employment (MBIE) in the framework of the Global Change Through Time research program (contract C05X1702).

## References

Becker, K. W., Lipp, J. S., Zhu, C., Liu, X.-L., & Hinrichs, K.-U. (2013). An improved method for the analysis of archaeal and bacterial ether core lipids. *Organic Geochemistry*, 61, 34–44. <https://doi.org/10.1016/j.orggeochem.2013.05.007>

Bernasconi, S. M., Daéron, M., Bergmann, K. D., Bonifacie, M., Meckler, A. N., Affek, H. P., et al. (2021). InterCarb: A community effort to improve interlaboratory standardization of the carbonate clumped isotope thermometer using carbonate standards. *Geochemistry, Geophysics, Geosystems*, 22(5), e2020GC009588. <https://doi.org/10.1029/2020gc009588>

Brassell, S. C., Eglington, G., Marlowe, I. T., Pflaumann, U., & Sarnthein, M. (1986). Molecular stratigraphy – A new tool for climatic assessment. *Nature*, 320(6058), 129–133. <https://doi.org/10.1038/320129a0>

Davtian, N., Bard, E., Ménot, G., & Fagault, Y. (2018). The importance of mass accuracy in selected ion monitoring analysis of branched and isoprenoid tetraethers. *Organic Geochemistry*, 118, 58–62. <https://doi.org/10.1016/j.orggeochem.2018.01.007>

Dearing Crampton-Flood, E., Tierney, J. E., Peterse, F., Kirkels, F. M. S. A., & Sinninghe Damsté, J. S. (2020). BayMBT: A Bayesian calibration model for branched glycerol dialkyl glycerol tetraethers in soils and peats. *Geochimica et Cosmochimica Acta*, 268, 142–159. <https://doi.org/10.1016/j.gca.2019.09.043>

De Jonge, C., Hopmans, E. C., Stadnitskaia, A., Rijpstra, W. I. C., Hofland, R., Tegelaar, E., & Sinninghe Damsté, J. S. (2013). Identification of novel penta- and hexamethylated branched glycerol dialkyl glycerol tetraethers in peat using HPLC-MS<sup>2</sup>, GC-MS and GC-SMB-MS. *Organic Geochemistry*, 54, 78–82. <https://doi.org/10.1016/j.orggeochem.2012.10.004>

De Jonge, C., Hopmans, E. C., Zell, C. I., Kim, J.-H., Schouten, S., & Sinninghe Damsté, J. S. (2014). Occurrence and abundance of 6-methyl branched glycerol dialkyl glycerol tetraethers in soils: Implications for palaeoclimate reconstruction. *Geochimica et Cosmochimica Acta*, 141, 97–112. <https://doi.org/10.1016/j.gca.2014.06.013>

De Jonge, C., Stadnitskaia, A., Hopmans, E. C., Cherkashov, G., Fedotov, A., & Sinninghe Damsté, J. S. (2014). In situ produced branched glycerol dialkyl glycerol tetraethers in suspended particulate matter from the Yenisei River, Eastern Siberia. *Geochimica et Cosmochimica Acta*, 125, 476–491. <https://doi.org/10.1016/j.gca.2013.10.031>

Ding, S., Schwab, V. F., Ueberschaar, N., Roth, V.-N., Lange, M., Xu, Y., et al. (2016). Identification of novel 7-methyl and cyclopentanyl branched glycerol dialkyl glycerol tetraethers in lake sediments. *Organic Geochemistry*, 102, 52–58. <https://doi.org/10.1016/j.orggeochem.2016.09.009>

Doeteler, S., Asifiwe, R. K., Baert, G., Bamba, F., Bauters, M., Boeckx, P., et al. (2021). Organic matter cycling along geochemical, geomorphic, and disturbance gradients in forest and cropland of the African Tropics – Project TropSOC database version 1.0. *Earth System Science Data*, 13(8), 4133–4153. <https://doi.org/10.5194/essd-13-4133-2021>

Häggi, C., Naafs, B. D. A., Silvestro, D., Bertassoli, D. J., Jr., Akabane, T. K., Mendes, V. R., et al. (2023). GDGT distribution in tropical soils and its potential as a terrestrial paleothermometer revealed by Bayesian deep-learning models. *Geochimica et Cosmochimica Acta*, 362, 41–64. <https://doi.org/10.1016/j.gca.2023.09.014>

Hopmans, E. C., Schouten, S., & Sinninghe Damsté, J. S. (2016). The effect of improved chromatography on GDGT-based palaeoproxies. *Organic Geochemistry*, 93, 1–6. <https://doi.org/10.1016/j.orggeochem.2015.12.006>

Hopmans, E. C., Weijers, J. W. H., Schefuß, E., Herfort, L., Sinninghe Damsté, J. S., & Schouten, S. (2004). A novel proxy for terrestrial organic matter in sediments based on branched and isoprenoid tetraether lipids. *Earth and Planetary Science Letters*, 224(1–2), 107–116. <https://doi.org/10.1016/j.epsl.2004.05.012>

Huguet, C., Hopmans, E. C., Febo-Ayala, W., Thompson, D. H., Sinninghe Damsté, J. S., & Schouten, S. (2006). An improved method to determine the absolute abundance of glycerol dibiphytanyl glycerol tetraether lipids. *Organic Geochemistry*, 37(9), 1036–1041. <https://doi.org/10.1016/j.orggeochem.2006.05.008>

Inglis, G. N., Collinson, M. E., Riegel, W., Wilde, V., Farnsworth, A., Lunt, D. J., et al. (2017). Mid-latitude continental temperatures through the early Eocene in western Europe. *Earth and Planetary Science Letters*, 460, 86–96. <https://doi.org/10.1016/j.epsl.2016.12.009>

Lauretano, V., Kennedy-Asser, A. T., Korasidis, V. A., Wallace, M. W., Valdes, P., Lunt, D. J., et al. (2021). Eocene to Oligocene terrestrial Southern Hemisphere cooling caused by declining  $p\text{CO}_2$ . *Nature Geoscience*, 14(9), 659–664. <https://doi.org/10.1038/s41561-021-00788-z>

Lu, H., Liu, W., Yang, H., Wang, H., Liu, Z., Leng, Q., et al. (2019). 800-kyr land temperature variations modulated by vegetation changes on Chinese Loess Plateau. *Nature Communications*, 10(1), 1958. <https://doi.org/10.1038/s41467-019-10978-1>

Martínez-Sosa, P., Tierney, J. E., Stefanescu, I. C., Dearing Crampton-Flood, E., Shuman, B. N., & Routson, C. (2021). A global Bayesian temperature calibration for lacustrine brGDGTs. *Geochimica et Cosmochimica Acta*, 305, 87–105. <https://doi.org/10.1016/j.gca.2021.04.038>

Naafs, B. D. A., Inglis, G. N., Zheng, Y., Amesbury, M. J., Bieser, H., Bindler, R., et al. (2017). Introducing global peat-specific temperature and pH calibrations based on brGDGT bacterial lipids. *Geochimica et Cosmochimica Acta*, 208, 285–301. <https://doi.org/10.1016/j.gca.2017.01.038>

O'Connor, L. K., Dearing Crampton-Flood, E., Jerrett, R. M., Price, G. D., Naafs, B. D. A., Pancost, R. D., et al. (2023). Steady decline in mean annual air temperatures in the first 30 k.y. after the Cretaceous-Paleogene boundary. *Geology*, 51(5), 486–490. <https://doi.org/10.1130/g50588.1>

Peterse, F., Prins, M. A., Beets, C. J., Troelstra, S. R., Zheng, H., Gu, Z., et al. (2011). Decoupled warming and monsoon precipitation in East Asia over the last deglaciation. *Earth and Planetary Science Letters*, 301(1–2), 256–264. <https://doi.org/10.1016/j.epsl.2010.11.010>

Peterse, F., van der Meer, J., Schouten, S., Weijers, J. W. H., Fierer, N., Jackson, R. B., et al. (2012). Revised calibration of the MBT-CBT paleotemperature proxy based on branched tetraether membrane lipids in surface soils. *Geochimica et Cosmochimica Acta*, 96, 215–229. <https://doi.org/10.1016/j.gca.2012.08.011>

Prahl, F. G., & Wakeham, S. G. (1987). Calibration of unsaturation patterns in long-chain ketone compositions for paleotemperature assessment. *Nature*, 330(6146), 367–369. <https://doi.org/10.1038/330367a0>

Raberg, J. H., Miller, G. H., Geirsdóttir, Á., & Sepúlveda, J. (2022). Near-universal trends in brGDGT lipid distributions in nature. *Science Advances*, 8(20), eabm7625. <https://doi.org/10.1126/sciadv.abm7625>

Rosell-Melé, A., Bard, E., Emeis, K.-C., Grimalt, J. O., Müller, P., Schneider, R. R., et al. (2001). Precision of the current methods to measure the alkenone proxy  $UK_{37}'$  and absolute abundance in sediments: Results of an interlaboratory comparison study. *Geochemistry, Geophysics and Geosystems*, 2(7), 2000GC000141. <https://doi.org/10.1029/2000gc000141>

Rosenthal, Y., Perron-Cashman, S., Lear, C. H., Bard, E., Barker, S., Billups, K., et al. (2004). Interlaboratory comparison study of Mg/Ca and Sr/Ca measurements in planktonic foraminifera for paleoceanographic research. *Geochemistry, Geophysics, Geosystems*, 5(4), Q04D09. <https://doi.org/10.1029/2003GC000650>

Schouten, S., Hopmans, E. C., Rosell-Melé, A., Pearson, A., Adam, P., Baurachs, T., et al. (2013). An interlaboratory study of  $TEX_{86}$  and BIT analysis of sediments, extracts, and standard mixtures. *Geochemistry, Geophysics, Geosystems*, 14(12), 5263–5285. <https://doi.org/10.1002/2013gc004904>

Schouten, S., Hopmans, E. C., Schefuß, E., & Sinninghe Damsté, J. S. (2002). Distributional variations in marine crenarchaeotal membrane lipids: A new organic proxy for reconstruction of ancient sea water temperatures? *Earth and Planetary Science Letters*, 204(1–2), 265–274. [https://doi.org/10.1016/s0012-821x\(02\)00979-2](https://doi.org/10.1016/s0012-821x(02)00979-2)

Schouten, S., Hopmans, E. C., van der Meer, J., Mets, A., Bard, E., Bianchi, T. S., et al. (2009). An interlaboratory study of  $TEX_{86}$  and BIT analysis using high performance liquid chromatography/mass spectrometry. *Geochemistry, Geophysics, Geosystems*, 10(3), Q03012. <https://doi.org/10.1029/2008gc002221>

Sinninghe Damsté, J. S. (2016). Spatial heterogeneity of sources of branched tetraethers in shelf systems: The geochemistry of tetraethers in the Berau River delta (Kalimantan, Indonesia). *Geochimica et Cosmochimica Acta*, 186, 13–31. <https://doi.org/10.1016/j.gca.2016.04.033>

Sinninghe Damsté, J. S., Ossebaar, J., Schouten, S., & Verschuren, D. (2012). Distribution of tetraether lipids in the 25-ka sedimentary record of Lake Challa: Extracting reliable  $TEX_{86}$  and MBT/CBT palaeotemperatures from an equatorial African lake. *Quaternary Science Reviews*, 50, 43–54. <https://doi.org/10.1016/j.quascirev.2012.07.001>

Sinninghe Damsté, J. S., Schouten, S., Hopmans, E. C., van Duin, A. C. T., & Geenevasen, J. A. J. (2002). Crenarchaeol: The characteristic core glycerol dibiphytanyl glycerol tetraether membrane lipid of cosmopolitan pelagic crenarchaeota. *Journal of Lipid Research*, 43(10), 1641–1651. <https://doi.org/10.1194/jlr.m200148-jlr200>

Speetjens, N. J., Tanski, G., Martin, V., Wagner, J., Richter, A., Hugelius, G., et al. (2022). Dissolved organic matter characterization in soils and streams in a small coastal low-Arctic catchment. *Biogeosciences*, 19(12), 3073–3097. <https://doi.org/10.5194/bg-19-3073-2022>

Tukey, J. W. (1977). *Exploratory data analysis*, Addison-Wesley series in behavioral science. Addison-Wesley Pub. Co.

Weijers, J. W. H., Schefuß, E., Schouten, S., & Sinninghe Damsté, J. S. (2007). Coupled thermal and hydrological evolution of tropical Africa over the last deglaciation. *Science*, 315(5819), 1701–1704. <https://doi.org/10.1126/science.1138131>

Weijers, J. W. H., Schouten, S., van den Donker, J. C., Hopmans, E. C., & Sinninghe Damsté, J. S. (2007). Environmental controls on bacterial tetraether membrane lipid distribution in soils. *Geochimica et Cosmochimica Acta*, 71(3), 703–713. <https://doi.org/10.1016/j.gca.2006.10.003>

Yang, H., Lü, X., Ding, W., Lei, Y., Dang, X., & Xie, S. (2015). The 6-methyl branched tetraethers significantly affect the performance of the methylation index (MBT') in soils from an altitudinal transect at Mount Shennongjia. *Organic Geochemistry*, 82, 42–53. <https://doi.org/10.1016/j.orggeochem.2015.02.003>

Yang, H., Xiao, W., Slowakiewicz, M., Ding, W., Ayari, A., Dang, X., & Pei, H. (2019). Depth-dependent variation of archaeal ether lipids along soil and peat profiles from southern China: Implications for the use of isoprenoidal GDGTs as environmental tracers. *Organic Geochemistry*, 128, 42–56. <https://doi.org/10.1016/j.orggeochem.2018.12.009>

Zech, R., Gao, L., Tarozo, R., & Huang, Y. (2012). Branched glycerol dialkyl glycerol tetraethers in Pleistocene loess-paleosol sequences: Three case studies. *Organic Geochemistry*, 53, 38–44. Advances in Organic Geochemistry 2011: Proceedings of the 25th International Meeting on Organic Geochemistry. <https://doi.org/10.1016/j.orggeochem.2012.09.005>